JOURNAL OF SPACECRAFT AND ROCKETS
Vol. 47, No. 1, January–February 2010

Engineering Notes

Drag Reduction for Spike Attached to Blunt-Nosed Body at Mach 6

R. Kalimuthu*
Vikram Sharabhai Space Center, Trivandrum 695 022, India
R. C. Mehta†
Nanyang Technological University, Singapore 639 798, Republic of Singapore
and
E. Rathakrishnan‡
Indian Institute of Technology, Kanpur 208 016, India

DOI: 10.2514/1.46023

Introduction

A HIGH-SPEED flow over a blunt body generates a bow shock wave in front of it, which causes a rather high surface pressure and, as a result, high aerodynamic drag. The surface pressure on the blunt body can be substantially reduced if a conical shock wave is generated by attaching a forward-facing spike. Thus, the introduction of the spike decreases the drag and increases the lift coefficient. The spike produces a region of recirculating separated flow that shields the blunt-nosed body from the incoming flow. The applicability of the spike is limited due to the possible appearance of flow oscillations in the separation region, which may reduce its positive effects and may cause aerodynamic disturbances during the flight [1].

Many experimental studies focused their attention on the influence of the spike's length on the aerodynamic characteristics of blunt bodies for various angles of attack at some transonic [2], supersonic [3–5], or even hypersonic [6–8] speeds. This Note contributes to the experimental study of the fluid flow structure and aerodynamic characteristics of a spike attached to blunt body at Mach 6. This Note analyzes the aerodynamic effects of the spike attached to the blunt body by using schlieren flow visualization and measured aerodynamic forces and moments.

This Note briefly describes the experimental results of the research on a hemispherical blunt nose body with and without spike at L/D ratio of 1.5 and 2 (where L is the spike length and D is cylinder diameter), and angle of attack α from 0 to 8 deg, with a 1 deg step. An in-depth description of the experiment conditions and results may be found in [9].

Experimental Facilities and Model Geometry

The hypersonic wind tunnel used for this study is an axisymmetric enclosed free-jet tunnel with a free-jet diameter of 0.254 m. This facility is of the pressure-vacuum type. The wind-tunnel system consists of high-pressure air supply, a pebble-bed heater, a contoured nozzle for delivering the flow at the required Mach number, a free-jet test section, a fixed-geometry diffuser with scoop to collect the nozzle flow, and the vacuum system. The facility is equipped with the state-of-the-art instrumentation system and required sensors. The hypersonic wind tunnel is designed for a Mach number range of 4–8.

Two force-measurement models were fabricated. The first one is the blunt body with a hemispherical nose and a cylindrical body. The diameter of the hemispherical cylinder D is 4.0×10^{-2} m and the length of the cylinder body is $1.25D$. The other model has a centrally located hole of diameter 4.0×10^{-3} m for fixing the spike. The dimensions of the hemisphere-spike body considered in the present investigation are depicted in Fig. 1. The spike consists of a hemispherical nose and a cylindrical part. The diameter of the cylindrical spike is $0.1D$. Spike lengths L of $1.5D$ and $2.0D$ were studied in the present experimental study.

Normal and axial force measurements were carried out with a six-component integral strain-gauge balance. Pressure measurements were made using a Scanivalve-type differential pressure transducer. The reference pressure was tunnel test-section plenum pressure, where the pressure was constant during testing time. Force measurements were made up to an 8 deg of angle of attack.

The freestream dynamic pressure of undisturbed flow, q, was taken as the reference value of pressure, the reference area A was the cross-sectional area of the cylindrical body of the model, and the reference length was its diameter D. The drag coefficient C_D and the lift coefficient C_L were calculated from the measured values of normal and tangential forces for the model without spike and with two different lengths of spikes. The pitching moment C_M was measured about the nose of spike. The fluid flowfield around the model was visualized using the schlieren technique. The fluid velocity, density, Mach number, dynamic pressure, and dynamic viscosity were calculated on the basis of stagnation pressure p_0, stagnation temperature T_0, static pressure p, and static temperature T. The settling chamber pressure and temperature were 8.3×10^5 Pa and 450 K, respectively. Reynolds number $Re_L = 0.5 \times 10^6$ was based on spike length $L = 6.0 \times 10^{-2}$ m. Pressure measurement model was identical to the model for force measurement. There were 12 pressure taps identified as θ at an interval of 30 deg. In the azimuthal direction, ψ measurements were in the interval of about 10 deg. The angles θ and ψ are depicted in Fig. 1, where the pressure probes were located. Pressure measurements were carried out at zero angle of attack.

Results and Discussion

Figure 2a shows the schlieren picture for the blunt-nosed body without spike at Mach 6. The bow shock wave in front of the blunt body is very well captured, as seen in the figure. The shock standoff distance Δ is measured from the schlieren picture and compared with the theoretical results. The ratio of shock standoff distance [10,11] with hemispherical diameter D is

$$\frac{\Delta}{D} = \frac{2\varepsilon}{1 + \sqrt{\frac{8\varepsilon}{3}}} \tag{1}$$

where ε is the density ratio across the normal shock and can be calculated using the following expression [12]:

$$\varepsilon = \frac{(\gamma - 1)M_\infty^2 + 2}{(\gamma + 1)M_\infty^2} \tag{2}$$

where subscript ∞ represents the freestream condition. The value of Δ/D is calculated using the above equations and found to be 0.189

Received 17 June 2009; revision received 4 October 2009; accepted for publication 6 October 2009.

*Scientist/Engineer, Aerothermal Test Facilities Division.
†Senior Fellow, Department of Mechanical and Aerospace Engineering. Senior Member AIAA.
‡Professor, Department of Aerospace Engineering. Associate Fellow AIAA.

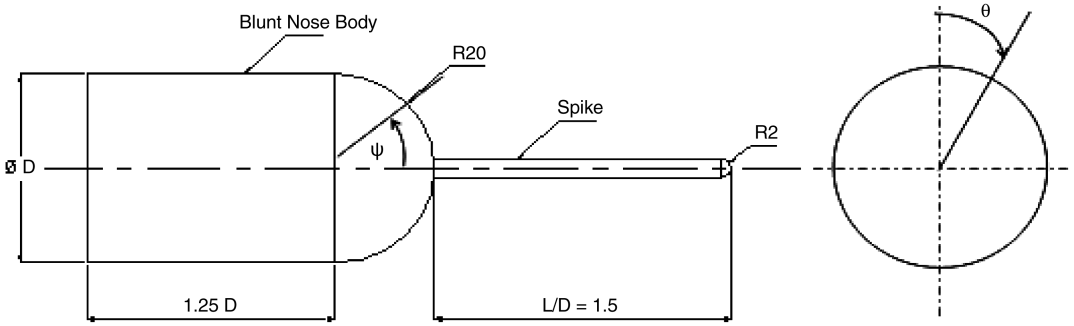

Fig. 1 Dimensions of the spiked blunt body.

and shows good agreement with the value obtained from the schlieren picture value of about 0.18.

The schlieren photographs of the model with the two different spike lengths are presented in Fig. 2 for $\alpha = 0$ and 5 deg. A strong influence of the spike on the fluid flowfield structure is evident in the schlieren pictures. High pressure behind the shock wave provokes boundary-layer separation. An approximately cone-shaped recirculation region is noticed between the shock wave and the spike due to the flow separation. There is a strong deflection of the flow in the zone of the boundary-layer reattachment on the blunt-nosed body, which depicts the appearance of a detached shock wave. As a result, the interaction of the wave with the shock wave emanating from the hemisphere cap of the spike can be visualized in the schlieren photographs (Figs. 2b–2e). The remainder of the flow structure appears identical to that for the body without a spike. The effect of angle of attack has altered the flow patterns, as seen in the schlieren pictures. The schlieren pictures reveal the flowfield behavior over the spike. The drag-reduction mechanism is due to the formation of a conical shock wave and the formation of a recirculating zone that envelops the spike. The increase of L/D ratio increases the recirculating zone in the windward side with the angle of attack. Motoyama et al. [8] also experimentally observed through the flow visualization technique at Mach 7 that a bow shock wave generated ahead of the spike and a large recirculating zone enveloped the spike. In the case of $L/D = 2.0$, the extent of separated zone is higher than with $L/D = 1.5$, and hence the drag reduction is higher. The general characteristics of the flow patterns presented in Fig. 2 are also in accordance with the results of Motoyama et al. [8].

It can be seen from Figs. 3 and 4 that both the drag coefficient C_D and lift coefficient C_L increase with the angle of attack α with and without spike. Five repeated tests [9] were conducted in order to get the repeatability of the measured data. The repeatability test data were analyzed and showed error bands of $\pm 2.4\%$ in the lift and the drag coefficients. Numerical simulations [13] were carried out to

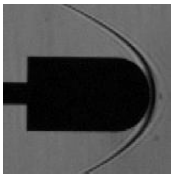

a) Hemispherical blunt body without spike, α = 0 deg

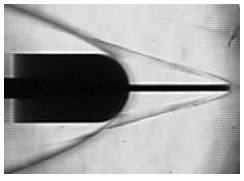

b) Spike with α = 0 deg and L/D = 1.5

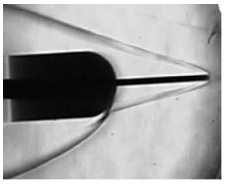

c) Spike with α = 5 deg and L/D = 1.5

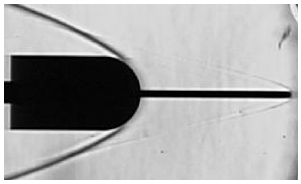

d) Spike with α = 0 deg and L/D =2.0

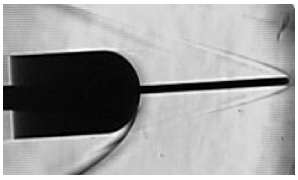

e) Spike with α = 5 deg and L/D = 2.0

Fig. 2 Schlieren photographs with and without spike.

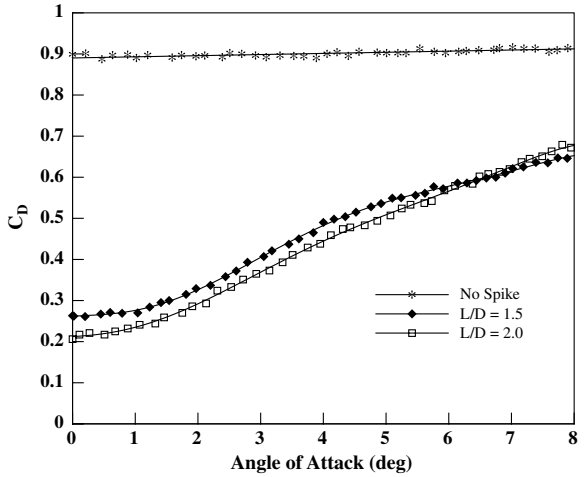

Fig. 3 Variation of drag coefficient with angle of attack.

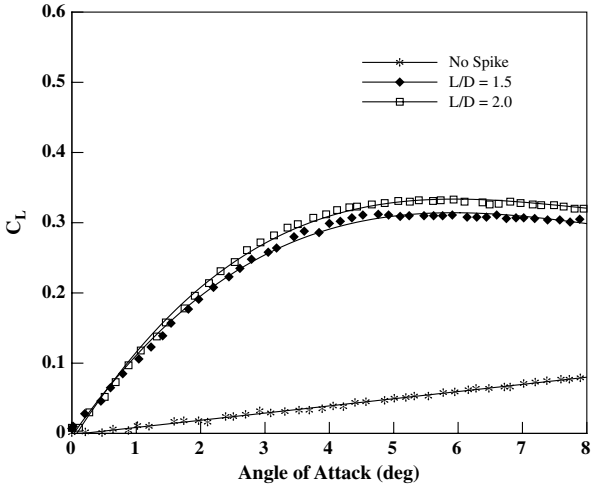

Fig. 4 Variation of lift coefficient with angle of attack.

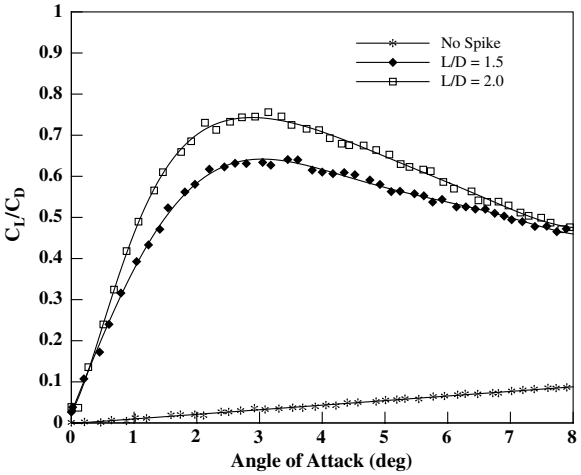

Fig. 5 Variation of lift to drag coefficient with angle of attack.

validate the experimentally measured drag coefficient at zero angle of attack at Mach 6. The maximum drag-coefficient difference between the experimental and the numerical results is found to be about 7%. Up to $\alpha = 6$ deg, $L/D = 2.0$ shows a higher drag reduction, and when $\alpha > 6$ deg, $L/D = 1.5$ shows a marginally higher drag reduction. When a spike is attached on the nose of a hemispherical-nosed body, a significant reduction of the C_D is found, as observed in Fig. 3. The influence of the spike length-to-diameter ratio can also be seen in the measured lift and drag coefficients. It is seen that the introduction of spike leads to reduction in the C_D as compared with the parental body. The C_D variation shows nonlinearity with respect to angle of attack. The maximum drag reduction for $L/D = 1.5$ is 62% at $\alpha = 0$ deg, and for $L/D = 2.0$ it is 78%. Drag-coefficient variation is not large beyond $\alpha = 6$ deg. Within the measurement range of angle of attack, the minimum drag reduction seen at $\alpha = 8$ deg for $L/D = 1.5$ is 26.7% and for $L/D = 2.0$ is 23%.

Figure 4 shows the lift-force-coefficient variation with angle of attack for hemisphere spikes of $L/D = 1.5$ and 2. For the blunt-nosed body without the spike, the lift coefficient shows almost a linear variation with respect to the angle of attack. Introduction of a spike at the nose of the blunt body leads to an increase of lift coefficient. This is due to the increased surface area of flow separation and higher pressure behind the shock wave of the spike on the configuration. The increase in lift coefficient C_L for $L/D = 1.5$ at $\alpha = 8$ deg is around 275% and for $L/D = 2.0$ is around 300%. Variations of the lift to drag coefficient with angle of attack for the parental body and hemispherical spike of $L/D = 1.5$ and 2.0 are

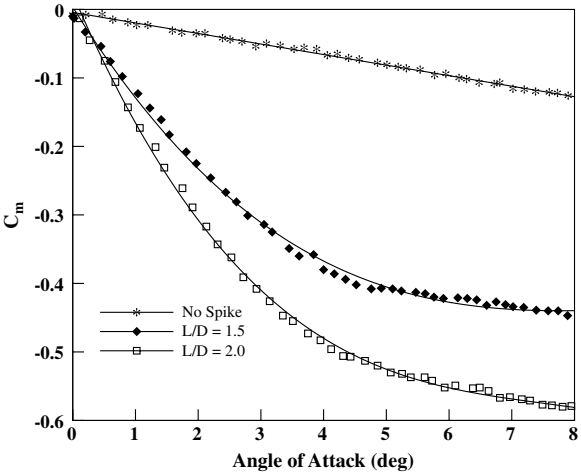

Fig. 6 Variation of pitching-moment coefficient with angle of attack.

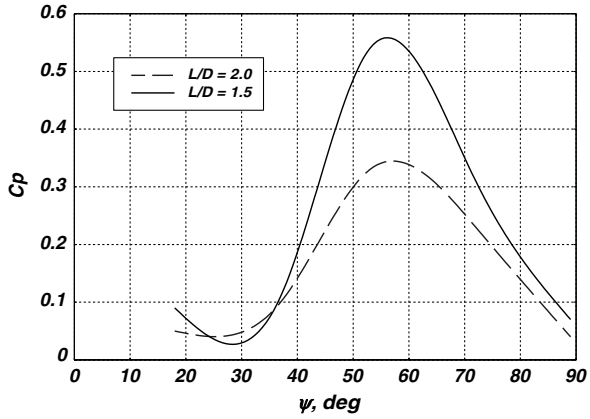

Fig. 7 Variation of pressure coefficient over the spike blunt-nosed body at zero angle of attack.

compared in Fig. 5. Within the measurement range of angle of attack the C_L/C_D has minimal variation beyond a 6 deg angle of attack. The maximum C_L/C_D is 0.78 at $\alpha = 3$ deg for $L/D = 2.0$.

Figure 6 shows the pitching-moment coefficient C_M with respect to angle of attack for the basic configuration and hemisphere spike. In the case of the blunt body without spike, the pitching-moment coefficient shows a linear variation with respect to the angle of attack. C_M variation is found to be nonlinear with the angle of attack for a hemisphere-spike configuration. The pitching-moment coefficient increases with the increasing L/D. The pitching-moment coefficient increase for $L/D = 1.5$ is about 275% and for $L/D = 2.0$ is 383%. Introduction of the spike shows the increasing trend of the pitching-moment coefficient. Thus, it shows that the model is going to become more stable. Therefore, more control force is needed to trim the vehicle.

The measured pressures are nondimensionalized with respect to dynamic pressure. The pressure coefficients are shown with spine curve fit in Fig. 7 for $L/D = 1.5$ and 2.0. The reduction of pressure is higher for $L/D = 2.0$. At $\psi = 50$ deg, the pressure rise is the maximum, which is attributed to the reattachment point of the flow. The pressure coefficient is less in the case of $L/D = 2.0$ as compared with the $L/D = 1.5$. It shows the influence of the spike length on the flow structure, as also observed in the schlieren pictures.

Conclusions

Flow visualization, force measurements, and pressure measurements on a blunt body with a hemispherical spike are carried out at Mach 6 in a hypersonic wind tunnel. The effects of the spike geometrical parameters on the drag, lift, pitching moment, and pressure measurements are studied experimentally. A forward-facing hemispherical spike attached to a hemispherical nose body significantly alters the structure of the flowfield and serves to reduce the drag coefficient by forming a recirculation region around the stagnation point of the blunt body. The drag coefficient is reduced to 62% for $L/D = 1.5$ and to 78% for $L/D = 2.0$. Consideration for compensation of increased pitching moment is needed. The surface pressure over the blunt-body in the presence of spike gives the maximum pressure at about 50 deg.

Acknowledgment

The authors express their sincere gratitude to the Referee and Associate Editor for giving the valuable comments, suggestions, and encouragement toward the improvement of the present work.

References

[1] Reding, J. P., Guenther, R. A., and Ritchter, B. J., "Unsteady Aerodynamic Consideations in the Design of a Drag-Reduction Spike," *Journal of Spacecraft and Rockets*, Vol. 14, No. 1, 1977, pp. 54–60. doi:10.2514/3.57160

[2] Koeing, K., Bridges, D. H., and Chapman, G. T., "Transonic Flow Modes of an Axisymmetric Blunt Body," *AIAA Journal*, Vol. 27, No. 9, 1989, pp. 1301–1302.
doi:10.2514/3.10262
[3] Chang, P. K., *Separation of Flow*, Pergamon, New York, 1970, pp. 469–530.
[4] Calarese, W., and Hankey, W. L., "Modes of Shock Wave Oscillations on Spike Tipped Bodies," *AIAA Journal*, Vol. 23, No. 2, 1985, pp. 185–192.
doi:10.2514/3.8893
[5] Milićev, S. S., Pavlović, M. D., Ristić, S., and Vitić, A., "On the Influence of Spike Shape at Supersonic Flow Past Blunt Bodies," *Facta Universitatis*, Mechanics, Automatic Control and Robotic, Vol. 3, No. 12, 2002, pp. 371–382.
[6] Bogdonoff, S. M., and Vas, I. E., "Preliminary Investigations of Spiked Bodies at Hypersonic Speeds," *Journal of the Aerospace Sciences*, Vol. 26, No. 2, 1959, pp. 65–74.
[7] Crawford, D. H., "Investigation of the Flow over a Spiked-Nose Hemisphere Cylinder at a Mach Number of 6.8," NASA TN D-118, 1959.
[8] Motoyama, N., Mihara, K., Miyajima, R., Watanuki, T., and Kubota, H., "Thermal Protection and Drag Reduction with Use of Spike in Hypersonic Flow," AIAA Paper 2001-1828, 2001.
[9] Kalimuthu, R., "Experimental Investigation of Hemispherical Nosed Cylinder with and Without Spike in a Hypersonic Flow," Ph.D. Thesis, Department of Aerospace Engineering, Indian Inst. of Technology, Kanpur, India, April 2009.
[10] Liepmann, H. W., and Roshko, A., *Elements of Gas Dynamics*, Dover, New Delhi, India, 2007.
[11] Truitt, R. W., *Hypersonic Aerodynamics*, Ronald Press, New York, 1959.
[12] "Equations, Tables and Charts for Compressible Flow," NACA Rept. 1135, 1953.
[13] Mehta, R. C., "Flowfield Computations over Conical, Disc and Flat Spiked Body at Mach 6," AIAA Paper 2009-0325, Jan. 2009.

M. Costello
Associate Editor